Role of pulmonary surfactant in airway closure: a computational study

D. R. OTIS, JR., M. JOHNSON, T. J. PEDLEY, AND R. D. KAMM
Department of Mechanical Engineering, Massachusetts Institute of Technology, Cambridge, Massachusetts 02139; and Department of Applied Mathematical Studies, University of Leeds, Leeds LS2 9JT, United Kingdom

OTIS, D. R., JR., M. JOHNSON, T. J. PEDLEY, AND R. D. KAMM. *Role of pulmonary surfactant in airway closure: a computational study.* J. Appl. Physiol. 75(3): 1323–1333, 1993.—A numerical model that simulates airway closure by liquid bridging during expiration has been developed. The effects of both surfactant and time-varying geometry have been included; the model determines the liquid layer flow resulting from a surface tension (Rayleigh) instability, and the computation traces the film's development to closure, yielding pressure, velocity, surface shape, and surfactant concentration distributions. It is found that surfactant is effective in retarding or eliminating liquid bridging through the reduction of the mean surface tension and the action of surface tension gradients. The former effect is also critical in minimizing the magnitude of the negative pressure in the liquid layer and thus presumably in reducing the tendency for airway compliant collapse.

airway edema; airway liquid; airway patency; computational model; gas trapping; liquid bridging; liquid plugging; residual volume; Rayleigh instability; surface tension

AIRWAYS IN THE LOWER REGIONS of the lung are known to close upon expiration to low lung volumes (5). The mechanisms responsible for airway closure, however, remain to be fully elucidated. Here, we consider one possible closure mechanism, that of liquid bridging (see Fig. 1), and simulate, by means of a theoretical model, the effect of pulmonary surfactant on closure during expiration. Lung volumes at closure are determined in a variety of circumstances.

Liquid bridging is caused by a surface tension instability of the thin liquid layer that lines the pulmonary airways. This layer prevents dehydration of the pulmonary epithelium and provides a pathway for the clearance of particles from the lung. The associated gas-liquid interface exhibits a surface tension that is altered by the presence of a surfactant secreted primarily by type II epithelial cells in the alveolar region (33). This surfactant is composed largely of phospholipids such as dipalmitoylphosphatidylcholine (DPPC) but also contains small amounts of protein (14, 30). An increase in surfactant concentration causes the surface tension to fall; in particular, a marked drop occurs during expiration, because the corresponding fall in the surface area of the liquid layer is accompanied by a rise in surfactant concentration. The surface tension approaches zero when the lung is deflated below ~60% of total lung capacity (TLC) (33). Although the amount of surfactant in the small airways is unknown, the existence of a continuous liquid layer would ensure its presence at some concentration; indeed, Macklem et al. (23) reported that the surface tension of the liquid lining the peripheral airways is similar to that in the air spaces.

Consider first what would be expected to happen during expiration if there is no surfactant present so that the surface tension is uniform. As lung volume falls, the radii of the airways are reduced, increasing the curvature of the air-liquid interface. This rise in curvature causes the negative pressure in the liquid to increase in magnitude. At the same time, tethering forces on the external surface of the airways fall because of the gradual relaxation of tension in the lung parenchyma. This combination of reduced inner wall pressure and relaxation of tethering forces decreases the effective transmural pressure of the airway and promotes the tendency of the airway to buckle, producing what is referred to as "compliant collapse."

A second mode of airway closure can also occur, particularly in diseased conditions that lead to accumulation of excess airway liquid. It has been observed (22) that a thin liquid layer on the inner wall of a small tube can undergo a fluid dynamic instability, leading to total obstruction of the tube by a liquid plug or "bridge," provided there is sufficient liquid present. This phenomenon is similar to the well-known Rayleigh instability (27), which causes a cylinder of liquid to break up into a sequence of droplets with lower aggregate surface area if the cylinder length exceeds its circumference. On the inner wall of a tube, the instability leads to the formation of a liquid bridge or an unduloid (see Fig. 1), depending on how much liquid is present. Unduloidal surfaces (7) are axisymmetric and possess constant mean curvature and lower surface area than the original cylinder; they will form if there is insufficient liquid to form a bridge. For tubes with length-to-diameter ratios in the range found in pulmonary airways, a bridge is formed if the amount of liquid in the tube (V_{liq}) is $>5.6s^3$, where s is the tube radius (22). If this condition is not met in a particular airway at TLC, it may be met after expiration to a lower lung volume with reduced airway radius. Recent in vitro experiments suggest that, given a liquid layer thickness of ~10 μm at TLC and a liquid layer instability that proceeds very rapidly, airway closure can take place at a lung volume of ~25% TLC, approximately equal to residual volume (RV) (22). Numerical simulations have also been performed, analyzing

0161-7567/93 $2.00 Copyright © 1993 the American Physiological Society

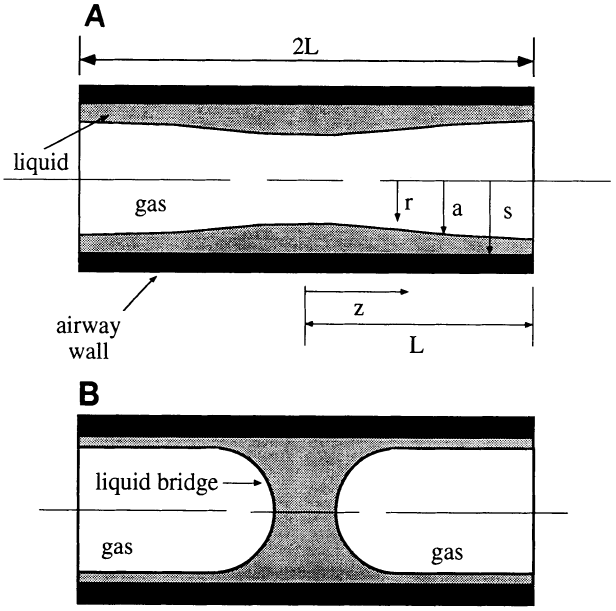

FIG. 1. Schematic of a sectioned airway showing airway liquid in unduloid (*A*) and liquid bridge (*B*) configurations. *a*, Radius to free surface; *r*, radial coordinate in airway; *s*, radius to airway wall; $h = s - a$ = film thickness; $2L$, airway length; $\xi = z/L(t)$ where z is axial coordinate in airway and t is time.

the process of liquid bridge formation (20, 21) and suggesting that the time scale for this fluid dynamic instability is inversely proportional to the surface tension and small compared with the breathing period, provided that no surfactant is present.

In reality, both compliant collapse and liquid bridge formation will tend to occur simultaneously, although their relative importance will depend on local factors such as airway stiffness and liquid volume. Halpern and Grotberg (12) considered the additional role of airway compliance in liquid bridge formation; the results demonstrated that compliance could both augment the rate at which closure by liquid bridging takes place and cause it to take place at a higher lung volume. Both processes are more likely to occur in diseased lungs that have a surplus of airway liquid and/or species in the airway liquid that interfere with normal surfactant function (11, 14).

Otis et al. (25) analyzed the effect of surfactant on liquid bridge formation in airways of fixed dimension, whereas Halpern and Grotberg (13) treated a similar problem in a compliant airway. Here, we extend the theoretical model of bridge formation, developed for constant surface tension by Johnson et al. (20), to include surfactant effects in tubes, the dimensions of which fall with time, as occurs in airways during expiration. Predictions are thereby made of the time to airway closure and of absolute lung volume at closure for various expiration rates.

It will be shown that surfactant has two effects on the closure process. First, surfactant causes an overall reduction in surface tension as lung volume decreases. This reduction in tension does not affect the critical value of V_{liq}/s^3 necessary for bridge formation, but it does produce a substantial rise in the time scale for bridge formation. Thus lung volume will fall further before a bridge forms. Second, axial variations in concentration cause surface tension gradients that impede the movement of the liquid layer, reducing the lung volume at closure still further.

METHODS

A single airway is modeled as a circular cylinder (Fig. 1), the radius (s) and length ($2L$) of which are taken to decrease in proportion to the 1/3 power of lung volume (V_L) (16) but remain proportional so that airway shape is preserved

$$s = s_0(V_L/TLC)^{1/3} \quad (1)$$

$$L = L_0(V_L/TLC)^{1/3} \quad (2)$$

The airway dimensions are chosen to be typical of a terminal or respiratory bronchiole with initial radius s_0 = 0.025 cm, initial length $2L_0$ = 0.150 cm, and initial air-liquid interface radius a_0 = 0.024 cm, so that the initial film thickness $s_0 - a_0$ = 10 μm.

In the expiration simulations, we let V_L decrease from TLC linearly in time (Fig. 2)

$$\frac{V_L}{TLC} = 1 - \frac{t}{T_{exp}} \quad (3)$$

where T_{exp} is the hypothetical time it would take to empty the airway (and entire lung) of all air if no liquid layer were present; we performed simulations for values between 0.05 s (for a very fast expiration) and 5 s. Calculations terminate when closure takes place at $t = t_E < T_{exp}$, typically at V_L between 10 and 30% TLC, where t is time and t_E is time at which airway closes; we call the absolute lung volume at which closure occurs V_{LE} in reference to *point E* in Fig. 2.

The amount of liquid in the airway is taken to be constant over the time scale T_{exp} and has been set by the specification of a_0, L_0, and s_0, where a is radius to free surface. For closure to occur, two conditions must be satisfied: first, the Rayleigh condition (see introduction) will be met when $L > \pi a$, which for our parameters corresponds to

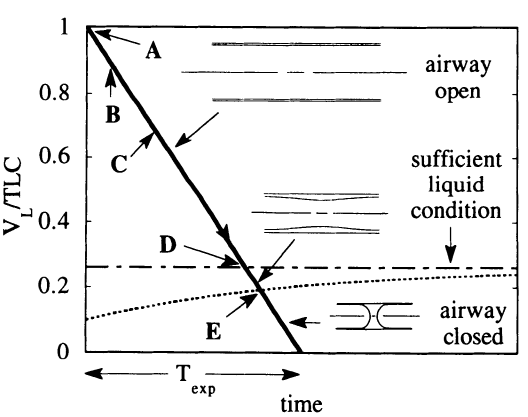

FIG. 2. Expiration modeled as linear decrease in lung volume (V_L) with time, starting from total lung capacity (TLC; at time = 0, from *A*). Rayleigh condition first satisfied at *B*; minimum surface tension first reached at *C*; sufficient liquid for closure condition first met at *D*; airway closure at *E*. Dashed curve shows schematically how lung volume at closure (V_{LE}) varies with T_{exp}; such a curve is an output of the model. Schematic of a sectioned airway is shown 3 times during expiration. a_0 = 0.024 cm, s_0 = 0.025 cm, L_0 = 0.075 cm, $\Gamma_0 = \Gamma_A$ = 1.0.

$$V_L/TLC < [1 - (a_0/s_0)^2]/[1 - (L_0/\pi s_0)^2] \quad (4)$$

Second, sufficient liquid must be available to form a bridge; this condition is met when the airway radius s decreases to the point where $V_{liq}/s^3 > 5.6$ so that

$$V_L/TLC < V_{liq}/5.6s_0^3 = 6\pi(1 - a_0^2/s_0^2)/5.6 \quad (5)$$

For the parameter values we have chosen, the Rayleigh condition is satisfied for V_L <89% TLC; that of sufficient liquid for closure is met for V_L <26% TLC.

Once these conditions are met, a bridge can form but takes a finite time to do so. If the expiration rate is relatively high, the lung will contract to a volume significantly <26% TLC before airway closure occurs. Alternatively, if the rate of bridge formation is high (due to high surface tension and/or low liquid viscosity) relative to the expiration rate, the bridge may form as soon as the conditions are met, i.e., at 26% TLC.

B and *D* in Fig. 2 are the points at which the Rayleigh and sufficient liquid for closure criteria, respectively, are satisfied. Closure takes place at *E*, and the dashed curve is the locus of *E* as T_{exp} is varied; such a curve is an output of the model and will depend on the surface tension behavior of the lining layer.

The liquid is taken to have density $\rho = 1$ g/cm^3 and viscosity $\mu = 0.01$ dyn·s·cm^{-2}, values close to those of water. These are reasonable values for the most peripheral airways because of the relative absence of mucus-secreting cells beyond the 15th generation (2). In simulations with variable surface tension, the surface tension at TLC is taken to be 30 dyn/cm, as in rat lungs at TLC (29).

It is assumed that the surfactant is concentrated in an insoluble monolayer at the air-liquid interface so that the total amount of surfactant in the interface remains constant. In the simulations, we solve for the local dimensionless surfactant surface concentration Γ and then assign a corresponding surface tension to this location through the relation shown in Fig. 3, based on data for DPPC (30); the data have been fit to a curve with the minimum surface tension set equal to 1 dyn/cm ($\gamma = \gamma_{min}$ = 1 dyn/cm for $\Gamma > \Gamma_C$). This minimum value, although not unrealistic, is arbitrarily chosen and could range between 0 and 5 dyn/cm.

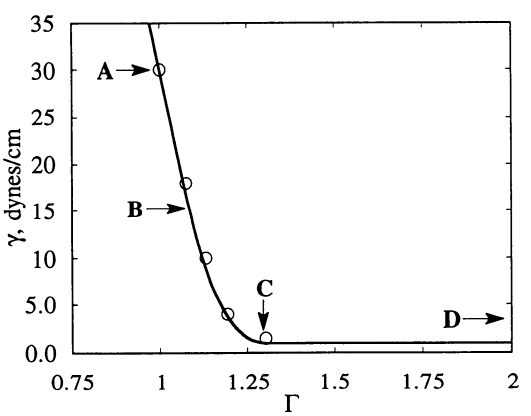

FIG. 3. Surfactant equation of state that yields surface tension γ for a given dimensionless surfactant surface concentration Γ. A curve is fit through data for dipalmitoylphosphatidylcholine (DPPC, ○) and is used as a model input. Minimum surface tension (γ_{min}) is taken to be 1 dyn/cm; surfactant concentration has been normalized with dimensional concentration corresponding to 30 dyn/cm, $\Gamma^* = 2.3 \times 10^{18}$ mol/m^2. *A–D* as in Fig. 2. DPPC data from Ref. 30. As $\Gamma \rightarrow 0$, $\gamma \rightarrow \gamma_{H_2O} = 72$ dyn/cm.

In Figs. 2 and 3, *A* is the start of the simulation at TLC, *B* is the Rayleigh condition first satisfied, *C* is the minimum surface tension value γ_{min} first reached, *D* is the sufficient liquid for closure condition first satisfied, and *E* is airway closure. The positions of these events on the curves are fixed by selection of the initial surface tension γ_A and the initial dimensions of the airway and liquid layer; in addition, the lung volume at *E* will vary with T_{exp}, but that at *B–D* will not. Each of the events identified by *A–E* corresponds to a point on the line in Fig. 2. However, spatial nonuniformities in surfactant concentration cause *B–E* each to be associated with a segment of the curve in Fig. 3; the arrows for *B* and *C* in Fig. 3 point to the mean surfactant concentration at times t_B and t_C, respectively. *A* is associated with a point in Fig. 3, because the surfactant concentration is initially uniform.

The dynamic equations governing the evolution of the liquid layer are set out in full in the APPENDIX. They represent conservation of liquid mass, conservation of surfactant, and conservation of liquid momentum (balancing fluid inertia, the pressure gradient driving the flow, the surfactant-induced shear stress, and the viscous resistance). Forces on the liquid layer caused by gravity are taken to be negligible in comparison to those caused by surface tension. The pressure in the liquid layer is a function of the interfacial curvature and tension and is calculated using a form of Laplace's law.

Calculation procedure. The basic equations were first manipulated to put them in the form most suitable for numerical computation; this process is described in the APPENDIX. Then the equations were integrated numerically by the technique employed by Johnson et al. (20).

The initial condition for each simulation was the same. The tube radius (s_0) was taken to have the value corresponding to TLC. However, the interface radius (a) was taken to be slightly nonuniform, equal to the appropriate initial undisturbed radius (a_0) plus a small sinusoidal perturbation of amplitude $0.001a_0$ and wavelength equal to the tube length $2L_0$, because nonuniformity of radius is necessary to trigger the growth of the instability. In nature or in a laboratory experiment, small fluctuations are ubiquitous and a perfectly cylindrical interface is never achieved; if an instability is possible, it will occur. A small initial perturbation must be specified, however, for computer simulations in which the expiration rate is zero; i.e., $T_{exp} \rightarrow \infty$. In such simulations, the time to closure decreases logarithmically with the perturbation amplitude. For simulations with finite expiration rates, a perturbation occurs naturally because of the wall movement, so that no initial perturbation need be specified. For the sake of uniformity, however, the same initial perturbation was used in all the simulations, regardless of expiration rate. The choice of a sinusoidal perturbation of wavelength equal to the length of the tube is most appropriate because, as the mean radius is reduced, an instability first becomes possible when the circumference $2\pi a$ falls below the length $2L$ and the wavelength of the disturbance that can then grow is indeed $2L$.

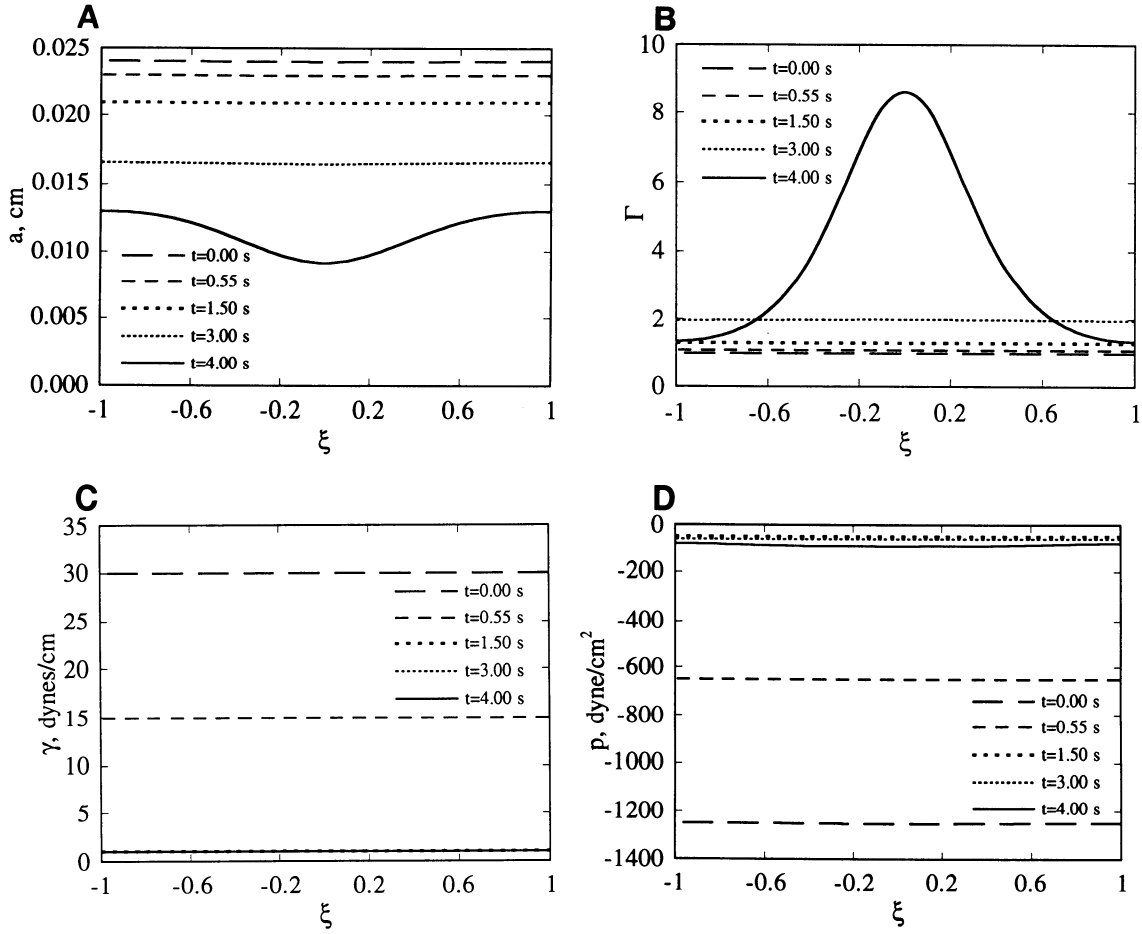

FIG. 4. Results for expiration with surfactant (variable surface tension). *A*: radius to air-liquid interface; *B*: dimensionless surfactant surface concentration; *C*: surface tension; *D*: liquid layer pressure (p; 980 dyn/cm^2 = 1 cmH_2O) vs. normalized axial position at t = 0.00, 0.55, 1.50, 3.00, and 4.00 s. T_{exp} = 5.00 s, Γ_0 = 1, t_B = 0.55 s, t_C = 1.54 s, t_D = 3.68 s, t_E = closure time = 4.07 s, V_{LE}/TLC = 0.186.

RESULTS

We first examine a relatively slow expiration, with T_{exp} = 5 s, starting at *A* in Fig. 2. The initial perturbation has set the radius a at the tube center (ξ = 0) to be less than that at the ends (ξ = ±1). For $t > t_B$, the Rayleigh condition is satisfied and so the minimum pressure is also at ξ = 0. This pressure distribution tends to drive liquid toward ξ = 0, causing the difference in film thickness between the tube ends and center to be magnified. However, these liquid velocities are initially very small relative to the airway contraction rate, so the interface remains nearly cylindrical and a decreases almost uniformly as the airway contracts, as shown in Fig. 4*A* for t < 3 s. Once $t > t_D$ = 3.68 s (or V_L/TLC < 0.264), the condition of sufficient liquid for closure has been met and a bridge can form; the finite rate of growth of the instability, however, causes bridge formation to lag behind this event and is completed at ξ = 0 after the lung has further contracted to $V_L = V_{LE}$ = 0.186TLC (at $t = t_E$ = 4.07 s).

As the airway contracts, the dimensionless surfactant concentration Γ rises, as shown in Fig. 4*B*; the flow toward ξ = 0 carries surfactant to that position, eventually making the maximum concentration there very evident. A rise in Γ causes the surface tension γ to fall through the relationship shown in Fig. 3. Figure 3 reveals that, for $\Gamma > \Gamma_C \approx 1.3$, the surface tension is constant at γ_{min} = 1 dyn/cm; hence the large gradient in Γ at t = 4 s (Fig. 4*B*) does not result in a surface tension gradient; instead, γ is uniform and equal to γ_{min}. The surface tension distribution for this and previous times is shown in Fig. 4*C*, revealing a 30-fold decrease in γ as Γ rises to Γ_C and higher values.

This large drop in γ makes the magnitude of the film pressure (p) drop, because γ and p are proportional. Moreover this reduction in the absolute value of p reduces the axial pressure gradient driving the flow, so the closure process is retarded. Figure 4*D* illustrates that the pressure is initially negative, of relatively large magnitude, and nearly constant at p = −1,250 dyn/cm^2. The magnitude of the pressure drops rapidly as the airway contracts, and once γ_{min} is reached at $t = t_C$, it increases a small amount with further contraction, because the surface curvature continues to increase while γ remains constant. The pressure profiles appear to be flat, but an axial pressure gradient exists and grows through the whole expiration; for $t > t_C$, the gradient drives liquid toward the low pressure at ξ = 0, causing velocity profiles like those shown in Fig. 5. These profiles show all the liquid in the airway flowing toward ξ = 0 and the velocity

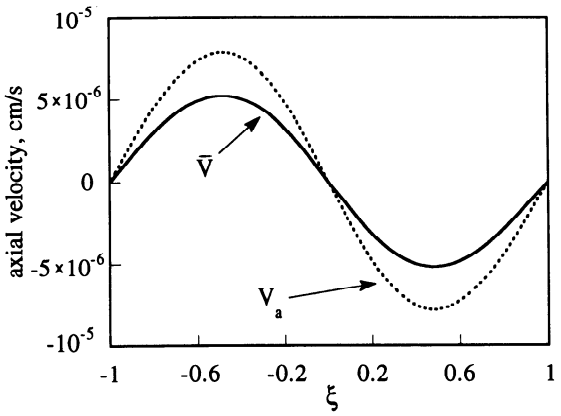

FIG. 5. Mean ($\bar{V}$) and surface (V_a) axial velocity vs. normalized axial position at $t = 1.55$ s > t_C. In the absence of surface tension gradient, surface velocity is 3/2 of mean and is directed toward point of lowest pressure ($\xi = 0$), as shown. For $t_B < t < t_C$, surface tension gradients exert tangential stresses on surface that are directed away from point of minimum pressure, tending to drag liquid away from this point and so retard closure process.

of the air-liquid interface ~3/2 of the mean, the expected value for the flow of a viscous layer of liquid with no stress applied at the interface $r = a$.

Although the concentration profiles in Fig. 4*B* also appear flat until $t = 3$ s, axial variations in concentration exist through the entire expiration, with the largest concentration at $\xi = 0$ because of surface contraction and convection. For $t < t_C$, this variation gives rise to minute surface tension differences between $\xi = 0$ and $\xi = \pm1$, on the order of 10^{-6} times the mean surface tension. Even a gradient of this magnitude, however, exerts a significant tangential force on the interface that can pull surface fluid from regions of low tension ($\xi = 0$) toward those of high tension ($\xi = \pm1$). Hence the surface tension gradient opposes the pressure gradient by impeding surface motion toward or causing flow away from the minimum pressure at $\xi = 0$. Once the surface tension reaches its minimum value at $t = t_C$, the gradient in surface tension disappears and the liquid velocities become as shown in Fig. 5. While it is present, the surface tension gradient tends to hinder flow toward $\xi = 0$ and so retard the closure process.

The surface tension gradient returns at the very end of the simulation, as can be seen by the decreasing concentrations at $\xi = \pm1$ between $t = 3$ and 4 s (Fig. 4*B*): convection toward $\xi = 0$ causes the surfactant concentration at the airway ends to eventually fall below Γ_C, making variations in surface tension reappear. However, because the liquid velocities near closure are very large, this late-appearing gradient acts for only a small fraction of the closure time and therefore has a minimal effect on the lung volume at closure.

If the surface tension is held constant at $\gamma = 1$ dyn/cm for the entire expiration, the interfacial shape profiles are quite similar to those obtained in the surfactant simulation (Fig. 4*A*) and $V_{LE} = 19.1\%$ TLC, slightly greater than the V_{LE} of 18.6% TLC obtained with surfactant. Figure 6*A* illustrates how a bridge develops if the surface tension remains constant at $\gamma = 30$ dyn/cm for the entire expiration. This relatively high tension accelerates the instability, causing closure at 26.3% TLC, immediately after the sufficient liquid for closure condition is met at $V_L = V_{LD} = 26.4\%$ TLC. This lung volume at closure is ~8% TLC greater than would have been obtained if surfactant were present. The negative pressure in the liquid layer, shown in Fig. 6*B*, is not moderated by a decreasing surface tension and so rises to large magnitudes as lung volume decreases.

Simulations of faster expirations for the same three surface tension conditions yield the results in Fig. 7, revealing that V_{LE} increases with increasing T_{exp} and surface tension. The V_{LE} values obtained with the variable surface tension nearly coincide with those obtained for γ = constant = $\gamma_{min} = 1$ dyn/cm, with a small difference that becomes apparent as $T_{exp} \rightarrow 5$ s. It is surprising that the variable surface tension condition yields a V_{LE} that is as low or lower than that obtained with $\gamma = \gamma_{min}$. This can be explained, however, in that, in the former case, a sur-

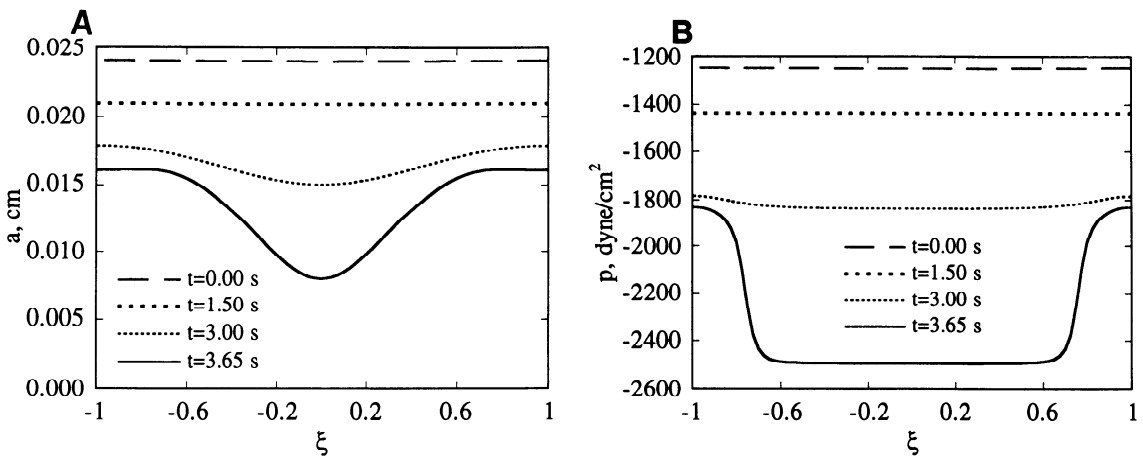

FIG. 6. Results for expiration with γ = constant = 30 dyn/cm. *A*: radius to air-liquid interface; *B*: liquid layer pressure vs. normalized axial position in airway at $t = 0.00$, 1.50, 3.00, and 3.65 s. Rate of growth of instability is higher than in surfactant case (Fig. 4) because of higher surface tension, and bridge is formed at nearly the highest lung volume allowed by sufficient liquid condition. As lung volume falls, increasing interfacial curvature causes negative pressure in liquid layer to increase in magnitude. Axial variations in a and p become apparent as instability grows. $T_{exp} = 5.00$ s, $t_B = 0.55$ s, $t_C = 1.54$ s, $t_D = 3.681$ s, t_E = closure time = 3.683 s, V_{LE}/TLC = 0.263.

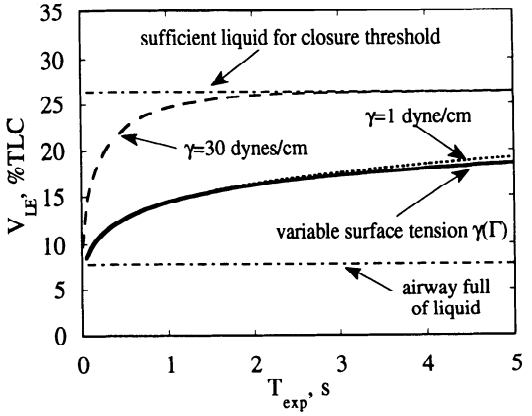

FIG. 7. Lung volume at closure as %TLC vs. T_{exp} for $h_0 = s_0 - a_0 = 10\ \mu m$. Results for constant surface tension ($\gamma = 1$ and 30 dyn/cm) and variable surface tension [$\gamma = \gamma(\Gamma)$ in Fig. 3] show that for $T_{exp} > 2$ s, a surface tension ≥30 dyn/cm will cause airway closure as soon as sufficient liquid for closure condition has been satisfied. Lower values of surface tension, made possible by surfactant, reduce V_{LE} significantly. Two horizontal lines mark limits of V_{LE} for given airway and liquid layer dimensions.

face tension gradient is operative for $t < t_C$ and counteracts the pressure gradient, which is small because large variations in curvature have not yet developed. Hence, for $t < t_C$, more flow in the direction of bridge formation has occurred in the $\gamma = \gamma_{min}$ case than in the variable surface tension case. For $t > t_C$, the surface tension conditions for the two cases are essentially identical, and, because bridge formation in the $\gamma = \gamma_{min}$ case has received a head start, it will have a slightly higher lung volume at closure.

As mentioned previously, all simulations were started with a radial perturbation of $0.001a_0$. If a larger value were used, the lung volume at closure would increase. However, for perturbation amplitudes ranging from 0 to $0.01a_0$, V_{LE} varies by ≤2.5% TLC about its mean value.

DISCUSSION

We have examined airway closure via a theoretical model of a liquid-lined tube, the dimensions of which change in a manner similar to that for a single pulmonary airway during expiration. The consequent reduction in airway volume causes the airway film to thicken, producing a situation in which small perturbations in film thickness can grow via the Rayleigh instability, eventually forming a meniscus that bridges the tube, producing airway closure.

Effects of pulmonary surfactant. These studies were undertaken to determine whether the presence of pulmonary surfactant in the small airways might play an important role in stabilizing the liquid layer and preventing airway closure in a model of a contracting airway. The results of these numerical simulations show that surfactant, at a concentration similar to that in the respiratory zone, can indeed influence the lung volume at which closure occurs by liquid bridging.

The curves in Fig. 7 reveal the effect of surface tension and expiration rate on V_{LE}. As $T_{exp} \rightarrow 0$, the rate of expiration is so great that the liquid layer instability has no time to act, and V_{LE} is independent of the surface tension, closure taking place when the airway is virtually full of liquid. As $T_{exp} \rightarrow \infty$, the expiration rate is so small that any liquid layer with a finite surface tension will form a liquid bridge as soon as the sufficient liquid for closure condition has been met. Between these two limits, the surface tension condition of the air-liquid interface will determine the lung volume at closure.

Figure 7 makes apparent the difference between V_{LE} calculated with a constant surface tension of 30 dyn/cm and that with a variable surface tension representative of pulmonary surfactant. For humans, physiologically realistic values of T_{exp} are ≥2 s. For 2 s < T_{exp} < 5 s, V_{LE} for γ = 30 dyn/cm is virtually flat near 26% TLC, whereas that for variable surface tension is ~10% TLC lower, ranging from 16 to 18% TLC. Hence surfactant, which makes variable surface tension possible, might eliminate liquid bridge formation if it reduced the lung volume at closure to a value less than that encountered in normal breathing. The expiration rate does not have a strong effect on V_{LE} for $T_{exp} \geq 2$ s, but if T_{exp} is increased sufficiently, V_{LE} for the variable surface tension and γ = 30 dyn/cm conditions will converge.

Surfactant reduces the lung volume at closure by two mechanisms. The principal means by which surfactant slows bridge formation is that of greatly reducing the mean surface tension as lung volume decreases. The large reduction in γ occurs because the surfactant is confined to the air-liquid interface and therefore is concentrated as the interface contracts during expiration. Figure 3 reveals that a concentration increase of 30% above the initial value causes the surface tension to fall from 30 dyn/cm to its minimum value, here taken to be 1 dyn/cm. Because the pressure is proportional to the surface tension, the 30-fold drop in tension causes a 30-fold reduction in the pressure gradient that drives the flow.

Surface tension gradients can also impede the growth of the instability. Perhaps their effect can best be appreciated by considering two extreme cases in a noncontracting tube in which the Rayleigh condition is satisfied and the amount of liquid is sufficient to form a bridge. (We consider a noncontracting tube to separate the surface tension gradient effect from that of the decreasing mean surface tension. The air-liquid interfacial area in a noncontracting tube does decrease during the closure process, but the mean surface tension stays very nearly constant.)

Consider first the case of no surfactant present. Once the interface is perturbed from its initial cylindrical geometry, the Rayleigh instability causes the perturbation to grow. Because no surface tension gradients are present, no tangential stress is exerted on the air-liquid interface, and the axial velocity of the surface is directed toward the minimum pressure, with magnitude equal to 3/2 of the mean value. This flow leads to the formation of a bridge in time t_1.

Alternatively, if the air-liquid interface is coated with a surfactant for which the surface tension is sensitive to changes in surface concentration and the mean surface tension is equal to the surface tension in the previous no-surfactant case, the flow leading to closure will create surface concentration gradients, with maximum concentration (and hence minimum surface tension) at the axial position where the bridge will form. The resultant sur-

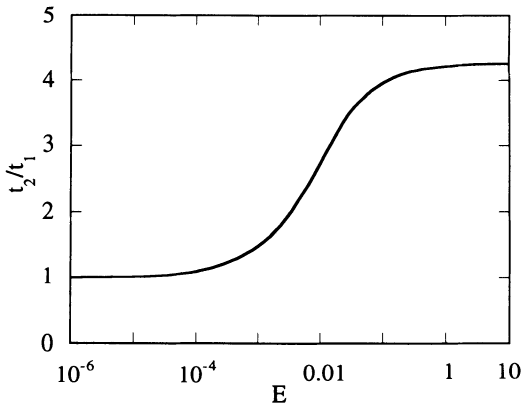

FIG. 8. Closure time (t_2) vs. Gibbs elasticity (E). t_1, Closure time when no surfactant is present. Results for noncontracting airway with a_0 = 0.020 cm, s_0 = 0.025 cm, L_0 = 0.075 cm, and mean γ = 20 dyn/cm.

face tension gradient exerts a tangential stress in the direction of greater surface tension, and so the flow leading to closure will be retarded. Therefore the closure time with surfactant, t_2, will be $>t_1$.

If the surface is stopped or "frozen" by gradients in the surfactant case, creating a zero-velocity condition at the air-liquid interface, $t_2/t_1 \approx 4$, because, for a given pressure gradient, the flow rate of a viscous fluid through a channel with two zero-velocity surfaces is one-fourth that with only one zero-velocity surface. If the slope of the surface tension vs. concentration relation is sufficiently steep (cf. Fig. 3, between *A* and *C*), the gradients can go beyond simply stopping the surface from moving and can, in fact, drive it in the direction opposite the mean flow. In this case, the time to closure can exceed $4t_1$.

A parameter that characterizes the slope of the surface tension vs. surfactant concentration in the neighborhood of its mean concentration is the Gibbs elasticity (E) (4), defined in dimensionless form as

$$E = -\frac{\Gamma^*_m}{\gamma_m}\left[\frac{\partial\gamma}{\partial\Gamma^*}\right]_{\Gamma^*_m} \qquad (6)$$

where Γ^*_m and γ_m are the mean dimensional surfactant concentration and mean surface tension, respectively. For DPPC, we used values of $\Gamma^*_m = 2.3 \times 10^{18}$ mol/m^2 (30) and γ_m = 30 dyn/cm, giving $E \approx 7$. Figure 8 shows how the time to closure (t_2) varies with E. For $E \geq 1$, there is the maximal surfactant effect, with the closure time more than four times greater than that for $E \leq 10^{-6}$, representative of no surfactant.

Figure 7 provides a comparison between the reduced mean surface tension and surface tension gradient effects. For T_{exp} = 5 s, the lung volume at closure with γ = 30 dyn/cm is 26.3% TLC; for $\gamma = \gamma_{min}$ = 1 dyn/cm, it is 19.1% TLC; and with variable surface tension with γ_A = 30 dyn/cm (Fig. 3), it is 18.6% TLC. The difference between the first two V_{LE} values is due solely to differences in mean surface tension. The much smaller difference between the last two values is caused chiefly by surface tension gradients. As mentioned previously, V_{LE} in the variable surface tension case is slightly less than that obtained with $\gamma = \gamma_{min}$, because surface tension gradients existing early in the expiration ($t < t_C$) effectively counter the pressure gradient at that stage, and no such mechanism impedes the flow when the surface tension is constant.

It was mentioned in RESULTS that the surface tension gradient can reemerge as closure approaches ($t \rightarrow t_E$). This is especially true if the surfactant experiences a maximum surface concentration Γ_{max} or "closest packing state" (3), which cannot be exceeded. We have performed simulations in which $\Gamma_{max} = \Gamma_C = 1.30$ (Fig. 3); the resultant lung volumes at closure are less than those shown in Fig. 7 for the variable surface tension condition (e.g., at T_{exp} = 5 s, V_{LE} = 17.1% TLC compared with 18.6% TLC), because the surface tension gradient is active for a larger fraction of the closure time near $t = t_E$. The effect is small and emphasizes the secondary importance of the surface tension gradient in slowing bridge formation.

If closure does not occur at end expiration when the surface tension is at its minimum value, it may occur early in inspiration, when the surface tension rises sharply. It is well known that, for a given interfacial area, the surface tension of pulmonary surfactant is greater during surface expansion than contraction (33). This causes the surface tension at a particular lung volume to be higher during inspiration than expiration (9). Indeed, Frazer and Weber (8) demonstrated that the most important factor in determining how much gas is trapped in an excised rat lung is the rate of inflation and not the rate of deflation. If liquid bridging is the mechanism responsible for closure and if no bridge has formed by end expiration, closure could take place during inspiration if the increased surface tension accelerated the instability enough to form a bridge. This would depend on the inspiration rate: if low, a bridge could form before lung volume was so great that the sufficient liquid for closure condition was no longer satisfied. This sensitivity to inspiration rate might explain the result of Frazer and Weber.

Airway closure in disease. The loss of normal surfactant function in the small airways due to *1*) impairment of surfactant production, *2*) interference with its surface tension-reducing capability [as would occur if plasma proteins invaded the airway film (14)], or *3*) restriction of surfactant movement from the respiratory zone to the small airways will result in increased surface tension in these same airways. This raised tension promotes airway closure at higher-than-normal lung volumes for a number of reasons.

First, Fig. 7 shows that, for a given expiration rate, an increased surface tension results in a higher lung volume at closure, because the increased tension accelerates liquid bridge formation.

Second, comparison of Figs. 4*D* and 6*B* shows that, at low lung volume (e.g., t = 3.65 s), the magnitude of the negative pressure tending to collapse the airway with constant surface tension $\gamma > \gamma_{min}$ is much greater than when surfactant function is normal (i.e., $\gamma = \gamma_{min}$). Although we have not included the effect of airway compliance in our model, this reduced transmural pressure would promote compliant collapse of the airway or a decrease in the lumen area, facilitating liquid bridge formation. Third, the accentuated negative pressure in the liquid layer may draw additional liquid from surrounding interstitial and capillary regions (or impede liquid transfer from the airways into those regions), causing the

liquid layer thickness to grow. As stated in the introduction, the greater the volume of liquid in the airway, the higher the lung volume at which closure can occur. In diseased conditions, the amount of airway liquid can increase markedly; for example, exposure to smoke has been found to increase the thickness of the mucus layer in the trachea by up to 10 times the normal value of 10 μm (17). Although the thickness and composition of the liquid layer in the peripheral airways of normal lungs are not known with certainty, it is believed that in all but the smallest airways the epithelium is lined with two layers of liquid: the first a periciliary fluid with depth equal to the length of the ciliary shafts ($\sim$6 μm) that lies beneath the second, composed of mucus. The mucus layer is believed to be contiguous in the large airways, with a depth of $\sim$5 μm; the layer coverage is less uniform in the smaller airways and disappears completely by the respiratory bronchioles (32). We have used a liquid layer thickness of 10 μm for airways in the terminal bronchial region at TLC and assumed it to be composed of the low-viscosity periciliary fluid because of the relative absence of mucus-secreting glands in the smallest airways. If a larger thickness were employed, the calculated V_{LE} values would rise accordingly.

Interpretation of V_{LE}. If liquid bridging plays a significant role in airway closure, we would expect that the calculated values of V_{LE} would correspond approximately to clinical values obtained for lung volume at closure and that factors that promote closure in the clinical setting would have a similar effect in the model. However, the clinical means used to ascertain whether closure has occurred are a subject of some debate. In addition, because of inhomogeneities in the lung, closure of individual airways likely occurs over a range of volumes, the mean value of which varies with age, height, sex, and possibly other factors (34).

It might seem most natural to compare V_{LE} with the closing capacity (CC), commonly believed to be the lung volume at which closure first occurs during a slow expiration from TLC to RV (34), hence the name. CC is measured by noting the lung volume at which phase IV begins in a nitrogen washout test (34). However, Hyatt et al. (18) and Rodarte et al. (28) demonstrated that CC increases with increasing expiration rate and may well be determined by regional flow limitation and not airway closure. Figure 7 reveals that V_{LE} decreases with increasing expiration rate, the opposite of the observed trend for CC. Moreover, CC values are significantly larger than the calculated V_{LE} values, despite our choice of an initial liquid layer thickness (10 μm) on the high end of the anticipated range in normal lungs. For example, the average CC for a 20-yr-old 1.8-m male is 32% TLC; for a 50-yr-old male of the same height, the mean CC is 46% TLC (34) compared with the largest V_{LE}, 26% TLC. For these reasons, the mechanism we have modeled does not seem to be that responsible for the onset of phase IV; therefore we conclude, as did Rodarte et al., that V_{LE} and CC result from different physical events.

On the other hand, there is reason to believe that the mechanism we have modeled may determine RV. The RV of an average 20-yr-old 1.8-m tall male is 26% TLC, comparable to the maximum V_{LE} we calculated. For a 50-yr-old male of the same stature, RV = 34% TLC (34). Our calculated V_{LE} values fall below these values but would tend to approximate them as additional factors that reduce the lumen area, such as airway compliance and excess airway liquid, are taken into account. Also the model formulation of constant expiration rate for the entire expiration ignores the fact that at low lung volume the flow rate will be limited by the maximal flow-volume envelope (34). The expiration rate at these low lung volumes is reduced, tending to shift the computed V_{LE} values upward, closer to typical RV values; the effect becomes more pronounced at higher expiration rates. Factors that are known to increase RV, such as excess airway secretions (as in chronic obstructive pulmonary disease) and increased airway compliance (as in emphysema), would also tend to increase V_{LE} (through increased liquid layer thickness and decreased airway radius, respectively).

It was pointed out above that the results presented in Fig. 7 are physiologically relevant in humans for T_{exp} greater than $\sim$2 s; in this range the lung volume at closure is not highly sensitive to expiration rate but is sensitive to the magnitude of the surface tension. This is consistent with the finding that additional air trapping in excised lungs (and hence, presumably, RV) is reduced by the presence of surfactant (6). While recognizing that other factors may contribute to airway closure, we conclude that the liquid bridging mechanism becomes more important as the airway lumen is increasingly obstructed and surfactant function is impaired and may contribute to the observed increase in RV in such cases (34).

Modeling considerations. Although every attempt was made to produce a model for airway closure that was realistic, as in any model, it was necessary to introduce various assumptions and approximations. Some of the more critical assumptions are discussed here.

One surfactant property not included in our model, that of surface shear viscosity, would tend to further stabilize the interface and delay or prevent bridge formation. Meban (24) determined that compression of pulmonary surfactant, as occurs during expiration, produces a sharp rise in surface shear viscosity, tending to retard surface movement. In the limit, this viscosity would immobilize the interface by making it solidlike (10) and so decrease the V_{LE} values in Fig. 7. The magnitude of this effect would be comparable to that caused by a surface tension gradient that hinders axial movement of the interface just before closure occurs. Calculations have shown that this effect can reduce V_{LE}/TLC by a few percent.

The lung volume at closure would be decreased still further if the minimum surface tension employed in the simulations was less than the 1 dyn/cm we used. Pattle (26) argued that the minimum surface tension is zero, in which case the lung volumes at closure we calculated would be overestimates and the actual values would be closer to that dictated by geometry alone (the limit for very low T_{exp} values in Fig. 7), provided compliant collapse does not occur. A lower minimum surface tension would also reduce the magnitude of the negative pressure in the liquid layer and therefore increase the effective

transmural pressure of the airway, making compliant collapse less likely.

We have assumed that the surfactant is confined to an insoluble monolayer so that its surface concentration increases without bound to many times its initial value as expiration proceeds, as in Fig. 4*B*. Many surfactant films experience a limiting or maximum concentration during film compression, however, reaching a "solid" state (1) in which further compression may result in complex behavior such as folding of the monolayer or desorption of surfactant. Although our insoluble monolayer approach would not be valid in these cases, such phenomena would not significantly alter the surface tension experienced at low lung volume during expiration; therefore we would not expect this aspect of surfactant function to have a large effect on the lung volume at closure.

We have taken the liquid layer viscosity to be equal to that of water, on the basis of a relative absence of mucus-secreting cells past the 15th generation of airways (2). There may be circumstances, however, that cause the viscosity of the liquid layer in the peripheral airways to increase, which would have the effect of prolonging liquid bridge formation and thus delaying or preventing closure. This assumes, however, that the conditions that lead to an increase in viscosity do not simultaneously produce a thicker liquid layer.

Stresses exerted on the air-liquid interface by gas in the peripheral airways were neglected because, during normal breathing, they are negligible compared with the maximum stresses caused by surface tension gradients. However, in the late stages of closure, when the airway is very narrow, and after closure, when it is blocked, shear and pressure forces exerted on the liquid by the airway gas would have to be taken into account to properly model bridge formation and movement. Also, gravity forces clearly become important relative to surface tension forces as the surface tension tends toward zero. Significant gravitational effects might *1*) cause more liquid to collect in the dependent regions of the lung, where closure is first observed and where the fraction of closed airways is highest (5), and *2*) lead to liquid pooling on the lower walls of the airways and thus alter the lung volume at closure.

The quantity of liquid lining an airway, V_{liq}, was taken to be constant during the expiration. The radial transfer of liquid through the airway wall can be estimated using measurements of pulmonary epithelial and endothelial hydraulic permeability (31) and indicates that the time scale for transepithelial flow of a quantity of liquid comparable to V_{liq} is much greater than T_{exp}. The axial intergenerational transfer of airway liquid is also considered to be negligible over T_{exp}. Support for this hypothesis has been provided by experiments in a branching network airway closure model in our laboratory, revealing no significant exchange of liquid between adjoining generations over the time scale required for a bridge to form.

An airway length-to-diameter ratio ($2L/2s$) of 3.0 was employed in all the simulations. Whereas a range of such ratios has been reported for the peripheral airways, the value we used falls near the upper bound of reported values. Ratios closer to 2.0 for the airways in the vicinity of the terminal bronchioles are more common (15); in these shorter tubes, the Rayleigh condition is met at a lung volume lower than that at which the condition of sufficient liquid for closure is met (so that $t_B > t_D$, the opposite of airways we have modeled, for which $L/s = 3.0$ and $t_B < t_D$), and the film thickness required to meet both conditions is greater than that in longer tubes; hence closure by bridging in shorter airways requires a thicker liquid layer.

It has been assumed in all the calculations that the airway retains a circular-cylindrical geometry during expiration, as shown in Fig. 1. In one extreme, that of a highly constricted airway, Yager et al. (35) reported that the peripheral airways have a rosette-shaped cross section and not a circular one. D. Yager (personal communication) found that the degree of this axial "folding" of the airway wall is much less in normal guinea pigs than in those with bronchoconstriction. However, this airway characteristic would need to be factored into the model in situations where the amplitude of the folds was comparable to or greater than the liquid layer thickness. In such a case, surface tension will cause the liquid to redistribute so that a more uniform curvature of the gas-liquid interface is attained. If the time scale for this redistribution is small compared with T_{exp} and if there is sufficient liquid in the airway to cover the epithelial folds and thus form a continuous liquid layer cuff, the thin-film dynamics leading to airway closure will be qualitatively similar to those in the simulations we have described.

In addition, D. Yager (personal communication) found that the average thickness of the airway lining layer in normal guinea pigs (which were frozen and then sectioned for measurement) actually decreases as lung volume is decreased from TLC to functional residual capacity. This runs contrary to our model assumption that the amount of liquid in the airway stays constant over T_{exp}, causing the liquid layer thickness to increase during expiration. Clearly, this emphasizes the need for a better understanding of how the liquid layer thickness varies during the breathing cycle and again suggests that the liquid bridging mechanism we have modeled may only occur in diseased lungs with significant excess airway liquid.

APPENDIX

The governing equations for conservation of mass, momentum, and species together with the boundary conditions for pressures and velocities are derived below. Where necessary, a transformation of coordinates is performed to facilitate calculations for the contracting airway.

Conservation of mass. For the axisymmetric incompressible liquid annulus under consideration (Fig. 1*A*) and neglecting liquid flux through the wall, the integral form of the continuity equation is

$$\left[\frac{\partial}{\partial t}(A)\right]_z = -\frac{\partial}{\partial z}(A\bar{w}) \qquad (A1)$$

where the subscript identifies which spatial coordinate is held constant in the partial differentiation with respect to time (for all spatial partial derivatives, time t is held constant and the subscript is omitted). z is the axial coordinate in the airway; $\bar{w}$ is the mean axial velocity in the annulus, in a fixed frame of reference

$$\bar{w} = \frac{\int_a^s w r dr}{\int_a^s r dr} \tag{A2}$$

where r is the radial coordinate in the airway; and

$$A = (s^2 - a^2)/2 \tag{A3}$$

which is proportional to the cross-sectional area of the liquid film. For simulations with contracting airways, we define a new spatial coordinate

$$\xi = z/L(t) \tag{A4}$$

which varies between -1 and 1 in the airway (see Fig. 1). A constant value of ξ corresponds to a fixed material point on the airway wall as the airway shrinks. In general

$$(\partial/\partial t)_z = (\partial/\partial t)_\xi - \frac{\xi \dot{L}}{L}(\partial/\partial \xi) \tag{A5}$$

and

$$(\partial/\partial z) = \frac{1}{L}(\partial/\partial \xi) \tag{A6}$$

where $\dot{L} = dL/dt$. We also introduce $\bar{V}(\xi,t)$, the mean fluid velocity relative to the moving wall at a given ξ

$$\bar{V} = \bar{w} - \xi \dot{L} \tag{A7}$$

so that *Eq. A1* can be rewritten as

$$\left[\frac{\partial}{\partial t}(A)\right]_\xi = -\frac{1}{L}\frac{\partial}{\partial \xi}(A\bar{V}) - \frac{A\dot{L}}{L} \tag{A8}$$

Conservation of surfactant. If we assume negligible transfer of surfactant between the surface and the adjacent liquid (as in an insoluble monolayer), negligible degradation of surfactant in the interface, and circumferential symmetry, the conservation of surfactant in the surface at $r = a$ may be expressed as

$$\left[\frac{\partial}{\partial t}(a\Gamma/\Psi)\right]_z = -\frac{\partial}{\partial z}(a\Gamma w_a/\Psi) + \frac{\partial}{\partial z}\left(aD_s\Psi\frac{\partial \Gamma}{\partial z}\right) \tag{A9}$$

where w_a is the axial velocity of the liquid layer at $r = a$, D_s is the surfactant surface diffusivity, and $\Psi = [1 + (\partial a/\partial z)^2]^{-1/2}$. Using the transformation in *Eqs. A4–A6*, we obtain

$$\left[\frac{\partial}{\partial t}(a\Gamma/\Psi)\right]_\xi = -\frac{1}{L}\frac{\partial}{\partial \xi}(a\Gamma V_a/\Psi) - \frac{a\Gamma\dot{L}}{L\Psi} + \frac{1}{L^2}\frac{\partial}{\partial \xi}\left(aD_s\Psi\frac{\partial \Gamma}{\partial \xi}\right) \tag{A10}$$

where $V_a = w_a - \xi\dot{L}$. *Equation A10* is "exact" in the sense that it holds equally well for small and large departures from the initial annular geometry.

Calculations have been performed with diffusion present, but even with an excessively large value of the surface diffusivity of 10^{-5} cm^2/s, compared with 2.4×10^{-5} cm^2/s for oxygen in water (19) and 10^{-7} cm^2/s for a myristic acid monolayer (1), diffusion had a negligible effect on the results.

Conservation of axial momentum. For axisymmetric flow with negligible body forces, the axial momentum equation is

$$\frac{\partial w}{\partial t} + u\frac{\partial w}{\partial r} + w\frac{\partial w}{\partial z} = -\frac{1}{\rho}\frac{\partial p}{\partial z} + \frac{\mu}{\rho r}\frac{\partial}{\partial r}\left(r\frac{\partial w}{\partial r}\right) + \frac{\mu}{\rho}\frac{\partial^2 w}{\partial z^2} \tag{A11}$$

where u is radial velocity. The airway liquid is taken to be Newtonian with constant viscosity. In the radial momentum equation, we make the thin-film approximation (20) and deduce that p does not vary significantly in the radial direction. Because the perturbation wavelength is long compared with the film thickness, the second viscous term is negligible compared with the first.

The velocity boundary conditions are

$$u_s = \frac{\partial s}{\partial t} + w_s\frac{\partial s}{\partial z} \tag{A12}$$

at the airway wall and

$$u_a = \frac{\partial a}{\partial t} + w_a\frac{\partial a}{\partial z} \tag{A13}$$

at the gas-liquid interface; the subscripts a and s refer to radial position. The no-slip condition at the airway wall gives

$$w_s = \xi\dot{L} \tag{A14}$$

and the condition matching the surface tension gradient in the air-liquid interface to the viscous shear stress in the liquid layer is

$$\mu(\partial w/\partial r)_a = -\frac{\partial \gamma}{\partial z} \tag{A15}$$

This neglects the effects of surface viscosity and surface shear imposed by airway gas and assumes that the perturbation is of very long wavelength (i.e., $\Psi \approx 1$). The boundary conditions at the airway center ($z = 0$) and ends ($z = \pm L$) are

$$(w)_{z=0} = 0 \tag{A16}$$

$$(w)_{z=\pm L} = \dot{L} \tag{A17}$$

The first condition is due to symmetry; the latter implies that there is no significant liquid flow through the bifurcations during a single expiration. To calculate $p(z,t)$, the pressure in the liquid film, we use Laplace's law as the normal stress boundary condition

$$p(z,t) - p_{gas} = \gamma\left[\frac{-\Psi}{a} + \frac{\partial}{\partial z}\left(\Psi\frac{\partial a}{\partial z}\right)\right] \tag{A18}$$

where p_{gas} is gas pressure. This law equates the pressure jump across the air-liquid interface to the product of the surface tension and the interfacial curvature. Surface viscosity has been omitted, and the gas core is assumed to be at constant p_{gas}.

Employing the boundary conditions at the airway wall and the air-liquid interface and using the integral technique of Johnson et al. (20), we can transform *Eq. A11* into

$$\left[\frac{\partial}{\partial t}(\bar{V})\right]_\xi + \frac{\bar{V}}{L}\frac{\partial \bar{V}}{\partial \xi} + \xi\dot{L} + \frac{\bar{V}\dot{L}}{L} = -\frac{1}{\rho L}\frac{\partial p}{\partial \xi} - \frac{4\mu\left\{\bar{V} + \frac{a}{2\mu L}\frac{\partial \gamma}{\partial \xi}\left[\frac{a^2\ln(s/a)}{A} - 1\right]\right\}}{\rho\left\{A - a^2\left[1 - \frac{a^2}{A}\ln(s/a)\right]\right\}} \tag{A19}$$

while the boundary conditions at the airway ends become

$$(\bar{V})_{\xi=0} = (\bar{V})_{\xi=\pm 1} = 0 \tag{A20}$$

Finally, the velocity at the air-liquid interface, required in the surfactant conservation equation, *Eq. A10*, can be shown to be

$$V_a = w_a - \xi\dot{L} = \frac{\left\{-2\bar{V} + \frac{a}{\mu L}\frac{\partial \gamma}{\partial \xi}\left[1 - \frac{a^2\ln(s/a)}{A}\right]\right\}}{A - a^2\left[1 - \frac{a^2}{A}\ln(s/a)\right]} \times [a^2\ln(s/a) - A] + \frac{a}{\mu L}\frac{\partial \gamma}{\partial \xi}\ln(s/a) \tag{A21}$$

Calculation technique. The approach of Johnson et al. (20) was employed to solve the coupled set of equations (*Eqs. A8, A10, and A19*), together with the specified boundary conditions

and the surfactant equation of state, in a simultaneous manner. A third-order Adams-Bashforth technique was used for the temporal derivatives, which were calculated explicitly, except for the viscous term, which was treated implicitly. Spatial derivatives were calculated using a central-differencing method, and the computational domain was the half-airway ($0 \leq \xi \leq 1$), with spatial discretization $\Delta z/L = \Delta\xi = 1/40$; no-flow conditions were imposed at $\xi = 0$ and $\xi = 1$ (see Ref. 20 for complete details).

We acknowledge the assistance of Dr. David Elad in certain aspects of the contracting airway analysis and the constructive comments of Drs. Jacob Bastacky, Jeffrey M. Drazen, David Edwards, Samuel Schürch, and Deborah Yager in various aspects of the study. Some calculations were performed on the Massachusetts Institute of Technology CRAY X-MP.

This work was supported by National Heart, Lung, and Blood Institute Grants HL-33009 and HL-45679 and by a grant from the Freeman Foundation.

Address for reprint requests: R. D. Kamm, Rm. 3-260, Massachusetts Institute of Technology, 77 Massachusetts Ave., Cambridge, MA 02139.

Received 20 March 1992; accepted in final form 24 April 1993.

REFERENCES

1. ADAMSON, A. W. *Physical Chemistry of Surfaces* (5th ed.). New York: Wiley-Interscience, 1990, p. 131–141.
2. CLARKE, S. W., AND D. PAVIA. Mucociliary clearance. In: *The Lung: Scientific Foundations,* edited by R. G. Crystal and J. B. West. New York: Raven, 1991, p. 1845–1859.
3. DJABBARAH, N. F., AND D. T. WASAN. Relationship between surface viscosity and surface composition of adsorbed surfactant films. *Ind. Eng. Chem. Fundam.* 21: 27–31, 1982.
4. EDWARDS, D. A., H. BRENNER, AND D. T. WASAN. *Interfacial Transport Processes and Rheology.* Boston, MA: Butterworth-Heinemann, 1991, p. 172.
5. ENGEL, L. A., A. GRASSINO, AND N. R. ANTHONISEN. Demonstration of airway closure in man. *J. Appl. Physiol.* 38: 1117–1125, 1975.
6. ENHORNING, G. Photography of peripheral airway expansion as affected by surfactant. *J. Appl. Physiol.* 42: 976–979, 1977.
7. EVERETT, D. H., AND J. M. HAYNES. Model studies of capillary condensation. I. Cylindrical pore model with zero contact angle. *J. Colloid Interface Sci.* 38: 125–137, 1972.
8. FRAZER, D. G., AND K. C. WEBER. Trapped air in ventilated excised rat lungs. *J. Appl. Physiol.* 40: 915–922, 1976.
9. FRAZER, D. G., AND K. C. WEBER. The effects of several gases (He, N_2, N_2O, and SF_6) on gas trapping in excised lungs. *Respir. Physiol.* 40: 323–333, 1980.
10. GOERKE, J., AND J. A. CLEMENTS. Alveolar surface tension and lung surfactant. In: *Handbook of Physiology. The Respiratory System. Mechanics of Breathing.* Bethesda, MD: Am. Physiol. Soc., 1986, sect. 3, vol. III, pt. 1, chapt. 16, p. 247–261.
11. HALL, S. B., R. H. NOTTER, R. J. SMITH, AND R. W. HYDE. Altered function of pulmonary surfactant in fatty acid lung injury. *J. Appl. Physiol.* 69: 1143–1149, 1990.
12. HALPERN, D., AND J. B. GROTBERG. Fluid-elastic instabilities of liquid-lined flexible tubes. *J. Fluid Mech.* 244: 615–632, 1992.
13. HALPERN, D., AND J. B. GROTBERG. Surfactant effects on fluid-elastic instabilities of liquid-lined flexible tubes: a model of airway closure. *J. Biomech. Eng.* In press.
14. HAWGOOD, S. Surfactant: composition, structure, and metabolism. In: *The Lung: Scientific Foundations,* edited by R. G. Crystal and J. B. West. New York: Raven, 1991, p. 247–261.
15. HORSFIELD, K. Morphometry of airways. In: *Handbook of Physiology. The Respiratory System. Mechanics of Breathing.* Bethesda, MD: Am. Physiol. Soc., 1986, sect. 3, vol. III, pt. 1, chapt. 7, p. 75–88.
16. HUGHES, J. M. B., F. G. HOPPIN, AND J. MEAD. Effect of lung inflation on bronchial length and diameter in excised lungs. *J. Appl. Physiol.* 32: 25–35, 1972.
17. HULBERT, W. C., B. B. FORSTER, W. LAIRD, C. E. PHIL, AND D. C. WALKER. An improved method for fixation of the respiratory epithelial surface with the mucous and surfactant layers. *Lab. Invest.* 47: 354–363, 1982.
18. HYATT, R. E., G. C. OKESON, AND J. R. RODARTE. Influence of expiratory flow limitation on the pattern of lung emptying in normal man. *J. Appl. Physiol.* 35: 411–419, 1973.
19. INCROPERA, F. P., AND D. P. DEWITT. *Fundamentals of Heat Transfer.* New York: Wiley, 1981, p. 785.
20. JOHNSON, M., R. D. KAMM, L. W. HO, A. SHAPIRO, AND T. J. PEDLEY. The nonlinear growth of surface-tension driven instabilities of a thin annular film. *J. Fluid Mech.* 233: 141–156, 1991.
21. KAMM, R. D., AND M. JOHNSON. Airway closure at low lung volume: the role of liquid film instabilities. *Appl. Mech. Rev.* 43, *Part* 2: S92–S97, 1990.
22. KAMM, R. D., AND R. C. SCHROTER. Is airway closure caused by a liquid film instability? *Respir. Physiol.* 75: 141–156, 1989.
23. MACKLEM, P. T., D. F. PROCTOR, AND J. C. HOGG. The stability of peripheral airways. *Respir. Physiol.* 8: 191–203, 1969.
24. MEBAN, C. Surface viscosity of surfactant films from human lungs. *Respir. Physiol.* 33: 219–227, 1978.
25. OTIS, D. R., JR., M. JOHNSON, T. J. PEDLEY, AND R. D. KAMM. The effect of surfactant on liquid film stability in the peripheral airways. *Adv. Bioeng.* 17: 55–57, 1990.
26. PATTLE, R. E. Properties, function, and origin of the alveolar lining layer. *Nature Lond.* 175: 1125–1126, 1955.
27. RAYLEIGH, LORD. On the instability of jets. In: *Scientific Papers of Lord Rayleigh.* New York: Dover, 1964, vol. I, art. 58, p. 361–371.
28. RODARTE, J. R., R. E. HYATT, AND D. A. CORTESE. Influence of expiratory flow on closing capacity at low expiratory flow rates. *J. Appl. Physiol.* 39: 60–65, 1975.
29. SCHÜRCH, S. Surface tension at low lung volumes: dependence on time and alveolar size. *Respir. Physiol.* 48: 339–355, 1982.
30. SCHÜRCH, S., H. BACHOFEN, J. GOERKE, AND F. POSSMAYER. A captive bubble method reproduces the in situ behavior of lung surfactant monolayers. *J. Appl. Physiol.* 67: 2389–2396, 1989.
31. TAYLOR, A. E., AND K. A. GAAR, JR. Estimation of equivalent pore radii of pulmonary capillary and alveolar membranes. *Am. J. Physiol.* 218: 1133–1140, 1970.
32. WANNER, A. Effects of methylxanthines on airway mucociliary function. *Am. J. Med.* 79, *Suppl.* 6A: 16–21, 1985.
33. WEIBEL, E. R. *The Pathway for Oxygen.* Cambridge, MA: Harvard University Press, 1984, p. 257–265, 317–325.
34. WEST, J. B. *Pulmonary Pathophysiology* (3rd ed.). Baltimore, MD: Williams & Wilkins, 1987, p. 14–18, 43, 204–205.
35. YAGER, D., J. P. BUTLER, J. BASTACKY, E. ISRAEL, G. SMITH, AND J. M. DRAZEN. Amplification of airway constriction due to liquid filling of airway interstices. *J. Appl. Physiol.* 66: 2873–2884, 1989.